

Inverse sampling intensity weighting for preferential sampling adjustment

Thomas W. Hsiao^{1*} Lance A. Waller¹

¹Department of Biostatistics and Bioinformatics,
Rollins School of Public Health,
Emory University

March 10, 2025

Abstract

Traditional geostatistical methods assume independence between observation locations and the spatial process of interest. Violations of this independence assumption are referred to as preferential sampling (PS). Standard methods to address PS rely on estimating complex shared latent variable models and can be difficult to apply in practice. We study the use of inverse sampling intensity weighting (ISIW) for PS adjustment in model-based geostatistics. ISIW is a two-stage approach wherein we estimate the sampling intensity of the observation locations then define intensity-based weights within a weighted likelihood adjustment. Prediction follows by substituting the adjusted parameter estimates within a kriging framework. A primary contribution was to implement ISIW by means of the Vecchia approximation, which provides large computational gains and improvements in predictive accuracy. Interestingly, we found that accurate parameter estimation had little correlation with predictive performance, raising questions about the conditions and parameter choices driving optimal implementation of kriging-based predictors under PS. Our work highlights the potential of ISIW to adjust for PS in an intuitive, fast, and effective manner.

Keywords: model-based geostatistics, preferential sampling, kriging, point process, inverse weighting

*Corresponding author: Thomas W. Hsiao, email: thsiao3@emory.edu

1 Introduction

The field of geostatistics comprises a set of methods to infer properties and predict unknown values (or functions) of a spatially continuous process $\{S(\mathbf{x}) : \mathbf{x} \in \mathcal{D} \subseteq \mathbb{R}^2\}$ from a discrete set of observation locations, denoted $\mathbf{X} = \{\mathbf{x}_1, \mathbf{x}_2, \dots, \mathbf{x}_n\}$. Model-based approaches estimated via maximum likelihood estimation (MLE) typically assume S is a realization from a random stochastic process, and subsequent inference and prediction treat \mathbf{X} as fixed (Diggle et al., 1998). This assumption further implies that the sampled locations are independent of the spatial process of interest, or in symbols, $[\mathbf{X}, S] = [\mathbf{X}][S]$, where square brackets indicate the probability distribution. Violations of this independence assumption are referred to as *preferential sampling* (PS). There is strong evidence to suggest neglecting PS can negatively impact both geostatistical inference and prediction (Diggle et al., 2010; Pati et al., 2011; Gelfand et al., 2012).

Early works in PS examined \mathbf{X} under the lens of a marked point process. Schlather et al. (2004) designed two Monte Carlo tests to detect dependence between marks and their locations. Ho and Stoyan (2008) introduced the classic PS adjustment model, referred to here as the *shared latent process* (SLP) model, and derived several of its properties. Full estimation and prediction procedures for the SLP model were formally established in the seminal work by Diggle et al. (2010).

The SLP framework induces dependence between the spatial process of interest and the sampling locations through a shared variable approach. Let μ, α, β , and τ^2 be scalars in \mathbb{R} , \mathbf{Y} denote the $n \times 1$ random vector of observed values sampled at locations \mathbf{X} , S the shared latent process, $S(\mathbf{X})$ the values of S evaluated at locations \mathbf{X} , IPP an inhomogeneous Poisson process, GP a Gaussian process, $C_\theta(\cdot, \cdot)$ a stationary covariance function indexed by parameter vector θ , and $\lambda(\cdot)$ the intensity function of \mathbf{X} conditional on S . Then the SLP model is as follows:

$$\begin{aligned}
[\mathbf{Y}|\mathbf{X}, S] &\sim N_n(\mu\mathbf{1}_n + S(\mathbf{X}), \tau^2 I_n), \\
[\mathbf{X}|S] &\sim IPP(\lambda), \\
\lambda(\mathbf{x}) &= \exp(\alpha + \beta S(\mathbf{x})), \\
S &\sim GP(0, C_\theta(\cdot, \cdot)).
\end{aligned}
\tag{1}$$

While the SLP framework has been extended to handle covariates in the mean model, non-Gaussian likelihoods, and multiple shared latent processes (Pati et al., 2011; Watson et al., 2019), for the purposes of illustration, we focus on the original formulation of a constant mean, Gaussian likelihood, and one shared latent process. Under the SLP model, sampling locations are no longer assumed to be fixed and are instead a realization from a log Gaussian Cox process (LGCP). The latent process S is assumed to follow a zero mean second order stationary Gaussian process (GP) and for the remainder of this paper, we further assume C_θ to be an isotropic Matérn covariance function. The SLP takes its name from the presence of S in both the mean model of \mathbf{Y} and the intensity function of \mathbf{X} . The parameter β can be interpreted as a single PS coefficient controlling the preferentiality of the SLP. The sign of β determines the direction of the preference, while its magnitude determines the likelihood of sampling extreme values.

Subsequent research on PS methods has remained largely faithful to the SLP model. Pati et al. (2011) extended the SLP model structure to a flexible Bayesian framework estimated by MCMC, and proved the posterior consistency of each of the mean, covariance and PS parameters under increasing domain asymptotics. Gelfand et al. (2012) also used Bayesian estimation, and introduced a framework to compare prediction surfaces under PS between different methods. A surprising finding from their simulation analysis was that inclusion of an informative covariate was not sufficient to correct for predictive bias. This empirical finding highlights the importance of the SLP model even when informative covariates explaining the dependence between \mathbf{X} and S are available. Dinsdale and Salibian-Barrera (2019) significantly improved the computational efficiency of the SLP model relative to the previous simulation-based methods by means of the stochastic

partial differential equations (SPDE) approach (Lindgren et al., 2011) combined with a Laplace approximation implemented in the Template Model Builder (TMB) R package (Kristensen et al., 2016). Watson et al. (2019) also fitted the SLP model using the SPDE approach but with an integrated nested Laplace approximation implemented in the R-INLA software (Rue et al., 2009), which enjoys comparable computational gains to the approach in Dinsdale and Salibian-Barrera (2019). The authors further defined a framework to model PS spatio-temporal data and better emulate the evolution of \mathbf{X} over time compared to the original SLP model defined in (1) above.

Several other contributions extend the SLP framework to explore a rich set of important applications, including air pollution monitoring (Lee et al., 2011, 2015), species distribution modeling (Manceur and Kühn, 2014; Fithian et al., 2015; Conn et al., 2017; Pennino et al., 2019; Gelfand and Shirota, 2019; Fandos et al., 2021), disease surveillance (Rinaldi et al., 2015; Cecconi et al., 2016; Conroy et al., 2023), phylodynamic inference (Karcher et al., 2016), hedonic modelling (Paci et al., 2020), bivariate spatial data (Shirota and Gelfand, 2022), spatially-varying PS (Amaral et al., 2023), optimal design under PS (Ferreira and Gamerman, 2015), space-filling designs (Ferreira, 2020; Gray and Evangelou, 2023), a hypothesis test to detect PS in spatio-temporal data (Watson, 2021), and exact Bayesian inference for the SLP model (Moreira and Gamerman, 2022; Moreira et al., 2023). The improved predictive ability and parameter estimation within the SLP framework contribute to the popularity of model-based approaches accounting for dependence between spatial processes and their observation locations.

While the benefits of the SLP structure and the ubiquity of PS data support its widespread adoption for spatial data analysis, the SLP model still contains significant limitations. Few software packages and out-of-the-box implementations exist for SLP estimation, often coming in the form of custom INLA or MCMC sampler code. Furthermore, the SLP model is challenging to integrate with modern spatial approximation techniques, many of which have become the standard in spatial data analysis due to their scalability and feasibility, offering computationally efficient alternatives to the MLE while maintaining high accuracy (Heaton et al., 2019). Among these methods, only the

SPDE approach has a well-documented implementation of a PS solution, and incorporating the SLP model into any other method would take a substantial effort. The SLP model requires joint evaluation of both the response and observation likelihood, not a trivial task. Prediction based on the SLP model also can suffer from high computational cost. While parameter estimation for the SLP model may scale well with the SPDE approach, prediction depends on summarizing the posterior distribution of $[S|\mathbf{X}, \mathbf{Y}]$ for each prediction point, which can be infeasible even on a moderately sized grid for both the Laplace approximation and MCMC.

An alternative strategy to the SLP is to incorporate dependence through the sampling intensities λ of the observations, rather than the entire likelihood of \mathbf{X} . These methods have been developed to much less fanfare compared to the SLP, and it remains unclear how well they work in geostatistical applications. The two main uses of sampling intensities are as a covariate in the mean model of \mathbf{Y} or as inverse weights in a likelihood adjustment (Vedensky et al., 2023). A potential advantage of sampling intensity methods is their robustness to the form of PS relative to the SLP framework, which addresses a very specific type of clustering process.

The biggest impediment to the use of the sampling intensity is the need to estimate this intensity from the observed locations, the driving reason such approaches have been sidelined in favor of full model-based approaches. Unlike in survey methodology where survey weights are fixed and known, sampling weights in geostatistical applications are largely unknown to the investigator and must be estimated. Unfortunately, nonparametric kernel smoothing estimators of the intensity (Diggle, 1985; Berman and Diggle, 1989) have few theoretical guarantees and are not consistent for the true intensity (Guan, 2008).

Even so, there is preliminary evidence that methods using nonparametrically estimated sampling intensities can still mitigate the effects of PS and, in some scenarios, can predict a surface better than the SLP approach in practice. Reich and Fuentes (2012) noted how the Bayesian SLP model parameters could be estimated without MCMC by replacing the shared latent process term in the mean model with some function of the sampling intensity $g(\lambda)$. Since the dependence between \mathbf{X} and S is completely con-

tained within $g(\lambda)$, the locations \mathbf{X} can once again be treated as fixed, so long as λ is estimated well. They show improved prediction using the sampling intensity covariate in a 1-dimensional kriging example. In another example, Zidek et al. (2014) provide an approach using estimated weights for air pollution monitoring. Instead of working in a continuous study region, however, these authors considered a finite superpopulation of possible sampling sites and the probability of selecting any site over time was modeled by a logistic regression. The estimated inverse probabilities were then used as weights in a Horvitz-Thompson style design-based estimator for unbiased estimation of parameters under PS. In a third example, Schliep et al. (2023) also considered a finite superpopulation and similarly deviated from traditional model-based geostatistics by using estimated sampling intensity weights to recover the estimated parameter values had the model been fit on the superpopulation, rather than estimate the parameters of the spatial process S . These authors also derived a kriging variance estimate adjusted for PS. Finally, Vedensky et al. (2023) conducted a simulation experiment comparing a univariate marginal composite likelihood (CL) weighted by inverse sampling intensities estimated by the `MASS::kde2d` function in R to the SLP and unweighted CL, and showed improved performance compared to no adjustment. We will refer to methods using inverse sampling intensities as weights in a weighted likelihood adjustment as *inverse sampling intensity weighting* (ISIW).

Despite preliminary investigations into ISIW for PS adjustment, specifics regarding the effectiveness of such approaches within model-based geostatistics remains largely unknown. In particular, it is unclear whether they reliably estimate both mean *and* covariance parameters for a latent spatial process on a 2D continuous surface. Composite likelihoods beyond pairwise difference and univariate marginal have also not been explored for ISIW. Finally, the robustness of ISIW and the SLP to misspecification has not been well-studied. In the sections below, we provide an expanded evaluation of ISIW methods, comparing the performance of MLE, SLP, and ISIW applied to the Vecchia and pairwise marginal CLs across multiple random fields and PS designs.

Our work proceeds as follows. We start off in Section 2 by providing background on

model-based geostatistics and introduce the key methods we use as a basis for ISIW. In Section 3, we present the implementation of ISIW in detail. In Section 4, we conduct a comparison analysis of the MLE, SLP, and ISIW through a set of simulation studies. In Section 5 we apply the same methods to the famous Galicia moss dataset which has been the dataset of choice when investigating PS. In Section 6 we finish with final remarks and discuss the implications of our work, and outline future directions for continuing investigation.

2 Model-based geostatistics

2.1 Estimation

2.1.1 Maximum likelihood estimation

Under non-preferential sampling (NPS), we define a model for the Gaussian observations \mathbf{Y} and underlying Gaussian process S following the SLP framework in (1), but we drop the point process likelihood for \mathbf{X} . The standard geostatistical model under NPS follows

$$\begin{aligned} [\mathbf{Y}|\mathbf{X}, S] &\sim N_n(\mu\mathbf{1}_n + S(\mathbf{X}), \tau^2 I_n), \\ S &\sim GP(0, C_\theta(\cdot, \cdot)). \end{aligned}$$

We further assume the covariance function C_θ follows a stationary isotropic Matérn covariance defined as

$$C_\theta(h) = \sigma^2 \frac{2^{1-\nu}}{\Gamma(\nu)} \left(\sqrt{2\nu} \frac{h}{\phi} \right)^\nu K_\nu \left(\sqrt{2\nu} \frac{h}{\phi} \right),$$

where $\theta := (\sigma^2, \nu, \phi)$ defines the covariance parameter vector containing the variance, smoothness, and range parameters respectively, h denotes the Euclidean distance between two points of observation, and K_ν is the modified Bessel function of the second kind. By convention, the smoothness parameter ν is assumed to be known and fixed *a priori* before estimation. Therefore, the parameters of interest are $\boldsymbol{\psi} := (\mu, \sigma^2, \phi, \tau^2)$.

Because any finite collection of random variables corresponding to point observations of S follows a multivariate Gaussian distribution and \mathbf{X} is treated as fixed, the observed

data likelihood is then defined by

$$[\mathbf{Y}, \mathbf{X}] \propto N_n(\mu \mathbf{1}_n, \Sigma_n(\theta) + \tau^2 I_n), \quad (2)$$

where Σ_n is the covariance matrix with ij th entry equal to $C_\theta(\|\mathbf{x}_i - \mathbf{x}_j\|)$. Estimation proceeds by optimization of the likelihood with respect to the parameter vector $\boldsymbol{\psi}$.

Justification for geostatistical inference via the MLE derives from spatial large sample theory. Two main frameworks have dominated asymptotics for geostatistical estimators: increasing domain asymptotics, and fixed domain (or infill) asymptotics. *Increasing domain asymptotics* assume that as $n \rightarrow \infty$, the study region \mathcal{D} expands, ensuring a minimum separation distance between observation locations and a fixed density of observations per unit area. *Fixed domain asymptotics*, on the other hand, keep \mathcal{D} fixed while increasing n , leading to a growing observation density and vanishing minimum distance between observations (i.e., observations occur closer together as the sample size increases within the fixed study area).

Under increasing domain asymptotics, the MLE for $\boldsymbol{\psi}$ is consistent and asymptotically normal (AN) (Mardia and Marshall, 1984; Bachoc, 2014, 2020). Results are more challenging under fixed domain asymptotics due to the inclusion of increasingly close observations of a spatially correlated process. Specifically, for a Matérn Gaussian process with known ν , only a subcomponent of the covariance parameters known as the *microergodic* parameter is consistently estimable and asymptotically normal (Zhang, 2004; Kaufman and Shaby, 2013). We refer to this parameter as κ , given by $\sigma^2/\phi^{2\nu}$ for Matérn covariance functions. The nugget τ^2 is also estimable (Tang et al., 2021) while the variance σ^2 and range ϕ are not (Zhang, 2004). Although the smoothness parameter ν is theoretically estimable, it is numerically challenging to estimate and is conventionally treated as fixed (Loh et al., 2021). Fixed effect coefficients in the mean are typically non-estimable (Wang et al., 2020), except under specific smoothness conditions on the covariates (Yu, 2022; Bolin and Wallin, 2024; Gilbert et al., 2024).

The main drawback for practical use of the MLE is its computational burden. Evalu-

ating the likelihood requires an inversion of the covariance matrix, which has $O(n^3)$ time and $O(n^2)$ space complexity making it infeasible for applications for moderately sized n . Recent advancement in modern spatial statistics has focused on GP parameter estimation using approximations which massively reduce computational burden in exchange for marginal decreases in efficiency. We explore composite likelihood and the Vecchia approximation, two approaches which have been widely adopted in geostatistics and are particularly conducive to weighting.

2.1.2 Composite likelihood

Sticking with our previous notation, let $\mathbf{Y} = (Y_1, Y_2, \dots, Y_n)^\top \in \mathbb{R}^n$ be a $n \times 1$ random vector with probability density $f(\mathbf{y}; \boldsymbol{\psi})$ for unknown r -dimensional parameter vector $\boldsymbol{\psi} \in \Psi \subseteq \mathbb{R}^r$. Define $\{\mathcal{A}_1, \dots, \mathcal{A}_K\}$ to be a set of K marginal or conditional events with associated likelihood $\mathcal{L}_k(\boldsymbol{\psi}; \mathbf{y}) \propto f(\mathbf{y} \in \mathcal{A}_k; \boldsymbol{\psi})$. The log composite likelihood (CL) is the weighted sum of the event-specific log likelihoods

$$\log \mathcal{L}_C(\boldsymbol{\psi}; \mathbf{y}) := \sum_{k=1}^K w_k \log \mathcal{L}_k(\boldsymbol{\psi}; \mathbf{y}),$$

where $\mathbf{w} := (w_1, \dots, w_K)$ is a vector of weights, not necessarily non-negative and the density f follows that defined in (2). The maximum CL estimate is defined as $\hat{\boldsymbol{\psi}}_C := \operatorname{argmax}_{\boldsymbol{\psi}} \log \mathcal{L}_C(\boldsymbol{\psi}; \mathbf{y})$. One common choice of CL is the univariate marginal where the log likelihood is the sum of the log marginal density of each observation.

$$\log \mathcal{L}_{UM}(\boldsymbol{\psi}; \mathbf{y}) = \sum_{i=1}^n w_i \log f(y_i; \boldsymbol{\psi}).$$

Typically, the use of this univariate marginal in geostatistics is limited because it ignores dependencies between observations and thus cannot estimate covariance parameters. For this reason, pairwise CLs have been much more popular (Varin et al., 2011). Bevilacqua and Gaetan (2015) compared the efficiency of three different pairwise CL estimators: pairwise marginal (PMLE), pairwise conditional (PCMLE), and pairwise difference (PDMLE) CLs. These authors concluded that the PMLE outperformed all other

pairwise CLs and recommended its use over the PCMLE and PDMLE. The likelihoods for each pairwise CL are

$$\begin{aligned}\log \mathcal{L}_{PM}(\boldsymbol{\psi}; \mathbf{y}) &= \sum_{i < j} w_{ij} \log f(y_i, y_j; \boldsymbol{\psi}), \\ \log \mathcal{L}_{PC}(\boldsymbol{\psi}; \mathbf{y}) &= \sum_{i \neq j} w_{ij} \log f(y_i | y_j; \boldsymbol{\psi}), \\ \log \mathcal{L}_{PD}(\boldsymbol{\psi}; \mathbf{y}) &= \sum_{i < j} w_{ij} \log f(y_i - y_j; \boldsymbol{\psi}).\end{aligned}\tag{3}$$

These authors also proved, under increasing domain asymptotics, the consistency and asymptotic normality of $\hat{\boldsymbol{\psi}}_C$ estimated from (3). Bachoc et al. (2019) proved the same properties for the PMLE and PCMLE in the one-dimensional setting under fixed domain asymptotics. However, the true utility of CL lies in its computational speed and robustness to misspecification. While the MLE requires a $O(n^3)$ matrix inversion and specification of the joint density, pairwise CL consists only of $O(n^2)$ terms and only requires correct specification of second order densities. The computational efficiency of pairwise CL can be further enhanced by using the weights \mathbf{w} to only include pairwise observations within a certain distance d apart (Bevilacqua and Gaetan, 2015).

In later sections, we will use the PMLE as a basis for ISIW due to its superior performance over other pairwise likelihoods. In particular, we do not consider the univariate marginal or PDMLE because they do not directly estimate the entirety of $\boldsymbol{\psi}$. In the next section, we discuss the Vecchia approximation, an alternative likelihood approach that achieves even greater computational and statistical efficiency than the CL.

2.1.3 Vecchia approximation

The Vecchia approximation is a specific case of CL based on the observation that the joint distribution can be decomposed as the product of conditional distributions. Let $\mathbf{Y} = (Y_1, \dots, Y_n)^\top \in \mathbb{R}^n$ and $p : \{1, \dots, n\} \rightarrow \{1, \dots, n\}$ be a permutation mapping which reorders \mathbf{Y} . We define the history of variable Y_j as a random subvector $\mathbf{Y}_{h(j)}$ where

$h(j) = \{l \in \{1, \dots, n\} : p(l) < p(j)\}$. The joint density of \mathbf{Y} can then be refactored as

$$f(\mathbf{y}; \boldsymbol{\psi}) = f(y_{p(1)}; \boldsymbol{\psi}) \prod_{i=2}^n f(y_{p(i)} | \mathbf{y}_{h(i)}; \boldsymbol{\psi}).$$

Vecchia observed that much of the information in the conditioning sets with higher indices was likely to be redundant. One could attain a good tradeoff of efficiency for computational gain by decreasing the size of each conditioning set and being judicious about which variables to include. The density would then be approximated as

$$f(\mathbf{y}; \boldsymbol{\psi}) \approx f_V(\mathbf{y}; \boldsymbol{\psi}) = f(y_{p(1)}; \boldsymbol{\psi}) \prod_{i=2}^n f(y_{p(i)} | \mathbf{y}_{q(i)}; \boldsymbol{\psi}), \quad (4)$$

where $q(i) \subseteq \{p(1), p(2), \dots, p(i-1)\}$ is the set of indices constituting the conditioning set of $y_{p(i)}$. The Vecchia estimate $\hat{\boldsymbol{\psi}}_V$ maximizes (4). The Vecchia approximation can also be written in a weighted CL form,

$$\begin{aligned} \log \mathcal{L}_V(\boldsymbol{\psi}; \mathbf{y}) &= w_1 \log f(y_{p(1)}; \boldsymbol{\psi}) \\ &+ \sum_{i=2}^n w_{1i} \log f(y_{p(i)}, \mathbf{y}_{q(i)}; \boldsymbol{\psi}) \\ &- \sum_{i=2}^n w_{2i} \log f(\mathbf{y}_{q(i)}; \boldsymbol{\psi}). \end{aligned} \quad (5)$$

While simple in concept, the Vecchia approximation requires careful selection of three key hyperparameters: 1) the size of the conditioning set, 2) which variables to include in each conditioning set, and 3) the ordering of the variables as determined by p . We denote the maximum size of any $q(i)$ as m . In all later sections, we choose $m = 20$ based on a clear case of diminishing returns in inference and prediction for $m > 20$ observed empirically in Datta et al. (2016). Default settings in two implementations of the Vecchia approximation (`GPvecchia` and `GpGp` R packages) are $m = 20$ and $m = 30$, respectively (Katzfuss and Guinness, 2021; Guinness, 2021). For the choice of which variables to include in the neighborhood $q(i)$, we follow the recommendation given in Vecchia (1988) by choosing the nearest neighbors to $y_{p(i)}$ measured by Euclidean distance. Ordering for the Vecchia approximation requires additional specification in multidimensional settings

due to the lack of natural ordering in observations of a spatial point process. We use the maxmin ordering scheme, which picks a location $p(i)$ sequentially by maximizing the distance to the nearest point in $\{y_{p(1)}, y_{p(2)}, \dots, y_{p(i-1)}\}$ and has been shown to approximate the true distribution better than other ordering methods (Guinness, 2018; Katzfuss and Guinness, 2021).

Theoretical justification of the Vecchia approximation in spatial statistics is relatively light compared to that of the MLE and CL. Typical approaches to proving fixed domain asymptotics fail due to the loss of stationarity in the parent process introduced by the Vecchia approximation (Zhang et al., 2024). However, it is impossible to deny its excellent empirical performance in applications (Heaton et al., 2019). A key advantage the Vecchia approximation possesses over typical CL is that (4) and (5) correspond to a valid joint probability distribution for \mathbf{Y} . As a result, the Kullback-Leibler (KL) divergence of the Vecchia approximation with respect to the true distribution can be computed and has been shown to be a nonincreasing function of m when the conditioning sets $q(i)$ are chosen as the nearest neighbors (Katzfuss et al., 2020; Huser et al., 2023).

The Vecchia approximation achieves a good balance of computational complexity and efficiency. It clearly outperforms other CL methods in terms of what order correlations are being accounted for, scalability, and probabilistic validity. This is the main reason for considering its use in ISIW methods compared to CL, a point we expand on in later sections.

2.2 Prediction

For many spatial analyses, the main goal is to predict values at unobserved locations. We focus on spatial prediction via *kriging*, or Gaussian process regression, a function approximation technique with point and variance estimate defined as

$$\begin{aligned}\hat{S}(\mathbf{X}_0) &= \mu + C_\theta(\mathbf{X}_0, \mathbf{X}_n)^\top \Sigma_n(\theta)^{-1}(\mathbf{Y} - \mu \mathbf{1}_n), \\ \text{Var}(\hat{S}(\mathbf{X}_0)) &= C_\theta(\mathbf{X}_0, \mathbf{X}_0) - C_\theta(\mathbf{X}_0, \mathbf{X}_n)^\top \Sigma_n^{-1}(\theta) C_\theta(\mathbf{X}_0, \mathbf{X}_n),\end{aligned}\tag{6}$$

where \mathbf{X}_0 represents unobserved locations to be predicted. In practice, since the parameters are unknown, all parameters in (6) are replaced with estimates obtained from any of the aforementioned or other estimation methods.

Kriging has several properties that make it an effective predictor of spatial surfaces. As the best linear unbiased predictor (BLUP), it minimizes mean squared prediction error among all unbiased predictors (Cressie and Wikle, 2015). However, it is important to note that this optimality no longer holds under preferential sampling, where even the true values of $\boldsymbol{\psi}$ used in the kriging equations yield suboptimal predictions (Dinsdale and Salibian-Barrera, 2019). Stein established the asymptotic efficiency of kriging under various robustness conditions (Stein, 1988, 1990a,b, 1993), while Wang et al. (2020) showed that kriging’s prediction error vanishes under a uniform metric. Additionally, Putter and Young (2001) demonstrated that the difference between predictions using kriging with estimated and the true parameters is asymptotically negligible if the joint Gaussian distributions of the spatial process under the true and estimated covariance functions are contiguous almost surely. Given these results, one could argue that the geostatistical model in (2) is more appropriate for spatial interpolation rather than inference.

3 Inverse sampling intensity weighting

We next describe estimation and prediction procedures of ISIW for PS adjustment. ISIW is a two-stage approach, wherein we first estimate the sampling intensity at each of the observation locations \mathbf{X} , and, in the second stage, we input the (estimated) inverse sampling intensities as weights into a weighted likelihood adjustment. The resulting adjusted parameter estimates are then substituted in the kriging equations for prediction.

3.1 Estimation of sampling intensity

The essence of ISIW is to account for the dependence between the response and observation locations by using the vector of estimated sampling intensities instead of the more complex full likelihood of the observation process. This approach assumes that

Table 1: Point process intensity function estimators considered in the simulation study.

Method	Reference	Bandwidth Selection
<code>diggle</code>	Diggle (1985)	Least-squares cross-validation
<code>scott</code>	Scott (1992)	Rule-of-thumb based on normal reference density
<code>ppl</code>	Loader (1999)	Likelihood cross-validation (leave-one-out)
<code>CvL</code>	Cronie and Van Lieshout (2018)	Maximum likelihood cross-validation
<code>CvL.adaptive</code>	van Lieshout (2021)	Adaptive bandwidth based on local point density
<code>R-INLA</code>	Simpson et al. (2016)	LGCP model (non-kernel-based)

the locations contain sufficient information about the spatial dependence structure of the observation locations to enable proper adjustment.

Methods to estimate a spatially varying intensity of a point process can be divided into parametric and nonparametric approaches. Domain knowledge can inform the parametric form of the intensity either through choice of model or covariates, but oftentimes this information is unavailable and nonparametric estimation is required. The nonparametric approaches follow the kernel smoothing approach discussed in Diggle (1985). Let k be a d -dimensional kernel function from $\mathbb{R}^d \rightarrow \mathbb{R}^+$, which is a symmetric probability density function. Given a bandwidth size $h > 0$ and edge correction factor $w_h(\cdot, \cdot)$, the nonparametric kernel smoothing estimator of the intensity function is given by

$$\hat{\lambda}(\mathbf{x}; h) = h^{-d} \sum_{\mathbf{y} \in \mathbf{X} \cap \mathcal{D}} k\left(\frac{\|\mathbf{x} - \mathbf{s}\|}{h}\right) w_h(\mathbf{x}, \mathbf{s})^{-1}, \mathbf{x} \in \mathcal{D}.$$

The key hyperparameter for nonparametric intensity estimation is the bandwidth size h . Bandwidth selection is a well-studied problem, with methods ranging from high bandwidth, smooth intensity estimators to low bandwidth, flexible intensity estimators. Each has its place in the bias-variance tradeoff, with higher bandwidths exhibiting higher bias with lower variance and lower bandwidths vice versa. We experiment with several bandwidth selection strategies implemented in the `spatstat` R package (Table 1).

The effectiveness of any ISIW approach for PS should improve the closer estimated weights $\lambda(\mathbf{x})^{-1}$ are to the true inverse intensities. In theory, a parametric LGCP model should estimate the true intensity better than any nonparametric estimator if \mathbf{X} follows a LGCP, especially with multiple realizations. However, it is known that it is impossible

to distinguish *between* a single realization from an inhomogenous Poisson process with deterministic intensity $\lambda(\mathbf{x})$ and *one from* a stationary Cox process whose conditional intensity coincides with λ (Gelfand et al., 2010). We consider a LGCP method introduced in Simpson et al. (2016) estimated by R-INLA to verify whether a known parametric model shows improvement over a nonparametric estimator.

Once the sampling intensities are estimated at every observation location, we calculate weights as the inverse of the sampling intensities and then normalize these to sum up to the number of observations n . The estimated weight for the i th observation becomes

$$\hat{w}_i = \hat{w}(\mathbf{x}_i) = n * \frac{\hat{\lambda}(\mathbf{x}_i)^{-1}}{\sum_{\mathbf{s} \in \mathbf{X}} \hat{\lambda}(\mathbf{s})^{-1}}. \quad (7)$$

3.2 Defining the likelihood

ISIW applies weights proportional to the inverse sampling intensity to each event in a likelihood factored as a product of densities. The only known examples of ISIW in the PS literature include a pairwise difference (Schliep et al., 2023) and univariate marginal CL (Vedensky et al., 2023). The pairwise difference CL cannot estimate μ directly, limiting ISIW’s impact on PS adjustment of the mean, while the univariate marginal CL cannot estimate covariance parameters θ . To address these gaps, we propose two new ISIW estimators for simultaneous mean and covariance estimation: the ISIW pairwise marginal (ISIW-PM) and ISIW Vecchia (ISIW-V) estimator. Let the weights be defined as in (7). Then the ISIW-PM follows

$$\log \mathcal{L}_{WPM}(\boldsymbol{\psi}; \mathbf{y}) = \sum_{i < j} w_i w_j \log f(y_i, y_j; \boldsymbol{\psi}).$$

For the ISIW-V, we initially considered weighting the likelihood as follows

$$\begin{aligned} \log \mathcal{L}_{WV}(\boldsymbol{\psi}; \mathbf{y}) &= w_{p(1)} \log f(y_{p(1)}; \boldsymbol{\psi}) \\ &+ \sum_{i=2}^n \left(\prod_{j \in \{p(i)\} \cup q(i)} w_j \right) \log f(y_{p(i)}, \mathbf{y}_{q(i)}; \boldsymbol{\psi}) \\ &- \sum_{i=2}^n \left(\prod_{j \in q(i)} w_j \right) \log f(\mathbf{y}_{q(i)}; \boldsymbol{\psi}), \end{aligned}$$

to maintain the probabilistic interpretation of the inverse weighting. However, numerical issues arise due to taking the product of several small weights, greatly increasing the chance of extreme values. As a more computationally efficient approach, we approximate the true weight using the following weighted Vecchia approximation

$$\begin{aligned} \log \mathcal{L}_{WV}(\boldsymbol{\psi}; \mathbf{y}) &= w_{p(1)} \log f(y_{p(1)}; \boldsymbol{\psi}) \\ &+ \sum_{i=2}^n w_{p(i)} \log f(y_{p(i)}, \mathbf{y}_{q(i)}; \boldsymbol{\psi}) \\ &- \sum_{i=2}^n w_{p(i)} \log f(\mathbf{y}_{q(i)}; \boldsymbol{\psi}). \end{aligned}$$

3.3 Numerical estimation

The ISIW for both the Vecchia and composite likelihood can be estimated by standard optimization procedures. In our study, we used the L-BFGS-B routine as implemented in the `optim` package in the R language. Initial values for parameters to be estimated were selected with general rules of thumb from the `GPVecchia` R package and all other optimization parameters were set to their default settings.

3.4 Winsorization of extreme weights

As with other inverse weighting procedures, a key concern for ISIW is extreme weights. Observation locations in sparsely sampled areas will have extremely high weights in the final likelihood and can cause numerical issues in the optimization. Two straightforward options are *trimming* and *Winsorization*. Trimming involves eliminating values considered as outliers, while Winsorizing enforces outliers to a threshold value. We chose

Winsorization to handle extreme values because trimming observations can remove rare information not captured by less extreme weights, weakening the effectiveness of PS adjustment. For our Winsorization procedure, we first normalize the sampling intensities $\hat{\lambda}$ to sum to n . We then Winsorized the normalized intensities by choosing a lower threshold (to be elaborated on later), and normalized the new resultant weights to sum to n .

3.5 Prediction

ISIW prediction of unobserved location follows by plugging in the estimated parameters $\hat{\psi}$ into the kriging equations in (6). This is a key distinction between ISIW and the SLP framework. Whereas prediction by ISIW adheres to kriging by substituting PS-adjusted parameters, the SLP model computes predictions from the estimated distribution of $[S|\mathbf{X}, \mathbf{Y}]$, making it much more computationally intensive.

4 Simulation analysis

4.1 Experiment

We conducted a simulation experiment to evaluate the inferential and predictive performance of ISIW-PM and ISIW-V versus the benchmark MLE and SLP approaches under preferential sampling. We generated $B = 500$ realizations for two separate Matérn random fields on a 200×200 grid on the unit square: a low-range ($\phi = 0.02$) and high-range ($\phi = 0.15$) surface with $\mu = 4$, $\sigma^2 = 1.5$, $\nu = 1$, and $\tau^2 = 0.1$. To test robustness of methods against a variety of observation patterns, we sampled three different point processes conditional on having $n = 100$ and $n = 800$ observations: a log Gaussian Cox process (LGCP), a sigmoidal Cox process (SCP), and a Thomas process. Traditionally, the SLP approach has only been tested against LGCP observation patterns where it is correctly specified.

The intensity function for the LGCP is $\exp\{\beta S(\mathbf{x})\}$. For the sigmoidal Cox process, the intensity function follows $\beta(1 + \exp\{-S(\mathbf{x})\})^{-1}$. For the Thomas process, a set of parent points was first generated from a homogeneous Poisson process. The number of

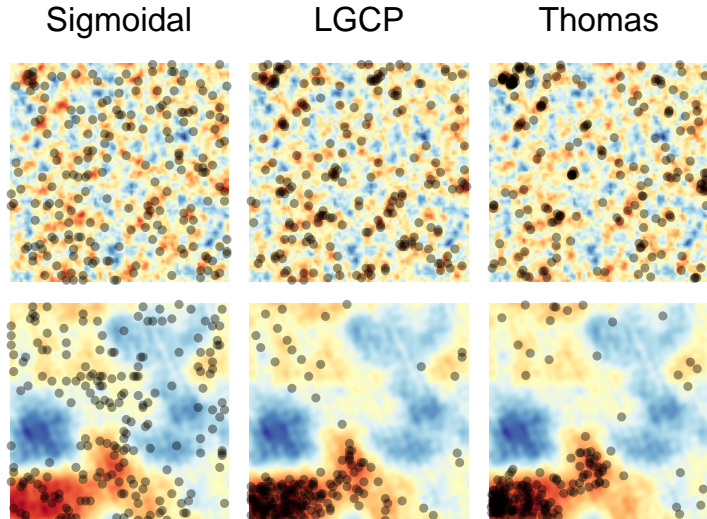


Figure 1: One realization of the point processes used in the simulation analysis for $n = 200$. The top and bottom row fields are low range ($\phi = 0.02$) and high range ($\phi = 0.15$) respectively.

offspring for each parent then followed a Poisson distribution with mean $\exp\{\beta S(\mathbf{x})\}$ and offspring points were sampled from a normal distribution centered at their respective parent locations, with a scale parameter of 0.1. We set $\beta = 1$ for all point processes. The SCP, LGCP, and Thomas process were deliberately selected to represent visually similar clustered point processes, ordered by increasing clustering intensity, with more distinct and separated clusters in the Thomas process (Figure 1).

For each set of observations, we fit the MLE, SLP, ISIW-PM, and ISIW-V models and compared the results in terms of parameter estimation and prediction. The MLE, ISIW-PM, and ISIW-V were estimated using `optim` as described in Section 3.3. We estimated the SLP model parameters using the INLA-SPDE implementation as defined in Watson et al. (2019) and used penalized complexity (PC) priors on the variance and range parameters (Simpson et al., 2017; Fuglstad et al., 2019). For the range parameter we set $P(\phi < 0.01) = 0.01$ and for the variance parameter we set $P(\sigma > 10) = 0.01$. The default priors for INLA were used for μ and τ , set as $N(0, 1000)$ and $\text{Gamma}(1, 5 \times 10^{-5})$, respectively. Prediction for the MLE and all ISIW methods followed the kriging equations, with point estimates of the requisite parameters substituted into (6).

We evaluated several variants of the ISIW methods, distinguished by their first-stage sampling intensity weight estimation (Table 1). As a gold standard for assessing the

optimal performance of ISIW, we also used the true weights extracted from the simulation surface, referred to as “Known” weights. The intensity estimators included multiple nonparametric kernel density estimators from `spatstat` and a parametric LGCP model, which used the same priors and mesh as the SLP. To determine a threshold for Winsorization, we conducted a small numerical experiment, simulating a Matérn random field with high range ($\phi = 0.15$) 100 times. For each replicate, we generated two LGCP point patterns with $\beta = 1$, one with $N = 100$ and the other with $N = 800$. ISIW-V was then fit under different weight thresholds using the `bw.diggle` bandwidth selection, as it was the most prone to numerical instability. The best-performing threshold, 1×10^{-2} , was selected based on yielding the best average root mean-squared prediction error (RMSPE). All subsequent ISIW methods implemented Winsorization using the 1×10^{-2} threshold.

Our approach to evaluating each method prioritized predictive performance due to the aforementioned challenges with standard statistical inference in fixed domain asymptotics and preferential sampling. The RMSPE was computed over each center point in a 200×200 grid, yielding 40,000 prediction points per method and simulation scenario. Parameter estimation was then assessed by computing relative bias and relative root mean-squared error (RMSE) for the parameter vector $(\mu, \sigma^2, \phi, \tau^2, \kappa)$.

4.2 Results

Across all simulation scenarios, INLA-SLP and ISIW-V Known were the top two predictors by RMSPE, with similar performance to each other and a clear margin over other methods. In general, INLA-SLP had better predictive performance in the high range scenario, whereas ISIW-V Known did so in the low range setting (Tables S1 and S2). The one exception was the high range scenario for the $N = 100$ Thomas process, where ISIW-V Known had both a lower RMSPE (0.694) and a lower standard deviation (0.15) compared to INLA-SLP (0.749 and 0.27) (Table S3). However, there were instances of predictive instability in INLA-SLP, as indicated by the high standard deviation of RMSPE, particularly in the $N = 100$ low range SCP and high range Thomas process $N = 100$ scenarios where INLA-SLP was misspecified. The ISIW methods also tended to

Table 2: Predictive performance of all sixteen methods based on median rank, mean rank, and percentage of total simulations when RMSPE for the method was lower than that of MLE and SLP. Rank was determined by RMSPE.

Method	Median Rank of RMSPE	Mean Rank of RMSPE	% RMSPE lower than MLE	% lower RMSPE than SLP
INLA-SLP	2	5.29	73.3	NA
ISIW-V Known	2	5.75	70.0	44.0
ISIW-V CvL.adaptive	5	6.53	72.7	31.8
ISIW-V diggle	5	5.96	78.5	29.3
ISIW-V CvL	7	7.38	85.0	28.9
ISIW-V ppl	7	7.37	74.4	27.8
ISIW-V INLA	8	8.23	74.0	27.9
ISIW-PM CvL.adaptive	8	8.01	65.1	28.3
ISIW-PM diggle	8	7.98	61.3	28.1
ISIW-V scott	9	8.29	85.6	28.4
ISIW-PM Known	9	8.60	51.8	23.9
ISIW-PM ppl	10	9.84	50.4	27.9
MLE	11	10.2	NA	26.7
ISIW-PM CvL	12	11.3	30.9	26.5
ISIW-PM INLA	14	12.3	27.0	24.9
ISIW-PM scott	14	12.7	22.3	24.6

run faster than the INLA-SLP at both sample sizes and had similar runtimes to the MLE (Table S4). We did not experiment with larger sample sizes than $N = 800$ because PS is primarily a concern in small to moderate sample sizes; as sample sizes grow sufficiently large, its effects diminish.

While ISIW-V using estimated weights did not match the predictive performance of ISIW-V Known, weight estimation variants including `diggle` and `CvL.adaptive` showed improved predictive performance over the alternative of no PS adjustment (Table 2). They achieved a median rank of 5 out of all 16 methods, had a lower RMSPE than MLE in over 70% of simulations, and even outperformed SLP nearly 30% of the time (for comparison, ISIW-V Known outperformed SLP in 44% of simulations). The `CvL` variant outperformed MLE in 85% of simulations, surpassing even SLP, which did so in 73%. Surprisingly, ISIW methods using weights estimated by the parametric LGCP model fitted in INLA performed relatively poorly, with a median rank of 8, though they still consistently outperformed MLE. All ISIW-V variants outperformed MLE in over 70% of simulations, whereas ISIW-PM lagged far behind, with some variants on average ranking

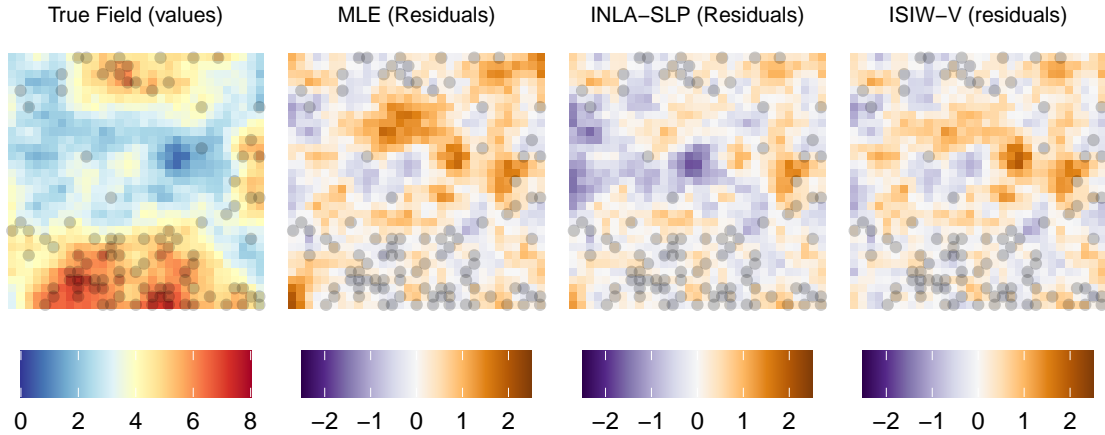


Figure 2: Example predictive surface for the MLE, INLA-SLP, and ISIW-V approaches. The first panel shows the true field values with observations denoted as points, while the remaining panels display residuals (observed minus predicted values) for each method.

worse than the MLE.

The variants that predicted best tended to estimate lower bandwidths which introduced greater noise in prediction, as reflected in the higher standard deviation of RMSPE for these variants. In contrast, `scott` and `ppl` traded variance for bias, which increased numerical stability but decreased the impact of weighting, making them nearly indistinguishable from prediction based on the MLE.

Figure 2 provides an illustrative example comparing the predictive tendencies of MLE, INLA-SLP, and ISIW-V Known. In the data-rich area at the bottom, predictions from all three methods are nearly identical. The differences emerge in data-sparse regions where PS is known to have its greatest impact. While the MLE overpredicts the center of the grid, the INLA-SLP predicts a much lower value over the same region which decreases predictive error but leads to underestimation in a specific area indicated by the deep purple. ISIW-V, similar to INLA-SLP, lowers predictions in that region but not as drastically, avoiding the central underprediction seen in INLA-SLP but still overestimating in another area, shown as dark orange slightly to the right of the center. As shown by this example, both INLA-SLP and ISIW-V adjust for PS in similar ways, but INLA-SLP tends to apply a larger adjustment in data sparse areas compared to ISIW-V.

Table 3 compares the relative bias and relative RMSE in parameter estimation for the MLE, SLP, and ISIW methods, with a specific focus on the Known, CvL, CvL.adaptive,

Table 3: Relative bias and RMSE in parameter estimation for MLE, SLP, and ISIW methods across all simulation scenarios. Bolded values indicate the method with the smallest bias or RMSE for a given parameter.

Method	Variant	μ		σ^2		ϕ		τ^2		κ	
		Bias	RMSE	Bias	RMSE	Bias	RMSE	Bias	RMSE	Bias	RMSE
MLE	-	0.106	0.173	0.046	0.589	0.013	0.429	-0.057	0.897	0.113	0.538
INLA-SLP	-	0.016	0.116	0.241	1.32	0.110	0.434	2.13×10^2	1.19×10^4	0.546	17.1
ISIW-V	Known	-0.259	0.409	0.035	20.8	90.9	4.52×10^3	0.053	1.72	0.712	1.58
	CvL	0.022	0.240	-0.057	1.10	65.1	2.71×10^3	-0.007	1.14	0.140	0.624
	CvL.adaptive	-0.018	0.268	0.362	51.9	1.25×10^3	3.08×10^4	0.441	2.44	2.44	1.14
	INLA	0.059	0.170	-0.068	0.807	-0.023	0.673	-0.013	1.15	0.166	0.804
ISIW-PM	Known	-0.161	0.309	-0.293	0.408	-0.352	0.489	0.713	1.09	1.900	7.65
	CvL	0.122	0.203	0.061	0.596	-0.168	0.397	0.871	1.50	0.885	2.05
	CvL.adaptive	0.042	0.150	-0.162	0.511	-0.184	0.630	0.782	1.35	1.550	11.0
	INLA	0.135	0.211	-0.018	0.570	-0.201	0.414	0.859	1.56	0.912	1.69

and INLA variants. While the MLE approach overestimated μ and INLA-SLP estimated μ accurately, ISIW-V Known significantly underestimated the mean by over 25% (averaging an estimate of three for a true mean of four), with a highly variable RMSE of 0.409. The estimated weight variants of ISIW-V had higher error in mean estimation compared to INLA-SLP but lower error than ISIW-V Known and MLE.

For the range parameter, ISIW-V estimates were consistently too high across all variants and exhibited potential numerical instability. In contrast, ISIW-PM underestimated the range but did so with much greater stability. MLE had relatively low estimation error for all covariance parameters, particularly κ and τ^2 , aligning with theoretical expectations. Aside from the mean, INLA-SLP did not estimate any parameter particularly well, with τ^2 showing significant numerical instability.

There was no clear relationship in the simulation between the method of parameter estimation and resulting predictive performance. INLA-SLP estimated the nugget and microergodic parameter extremely poorly, despite these being theoretically among the easiest to estimate, while ISIW-V on average underestimated the mean by 25% and vastly overestimated the range by more than a factor of 90. Yet, both methods led in predictive performance. In contrast, MLE and the CvL and INLA variants of ISIW produced relatively good parameter estimates but consistently ranked lower in predictive performance, with prediction errors far exceeding those of INLA-SLP and ISIW-V.

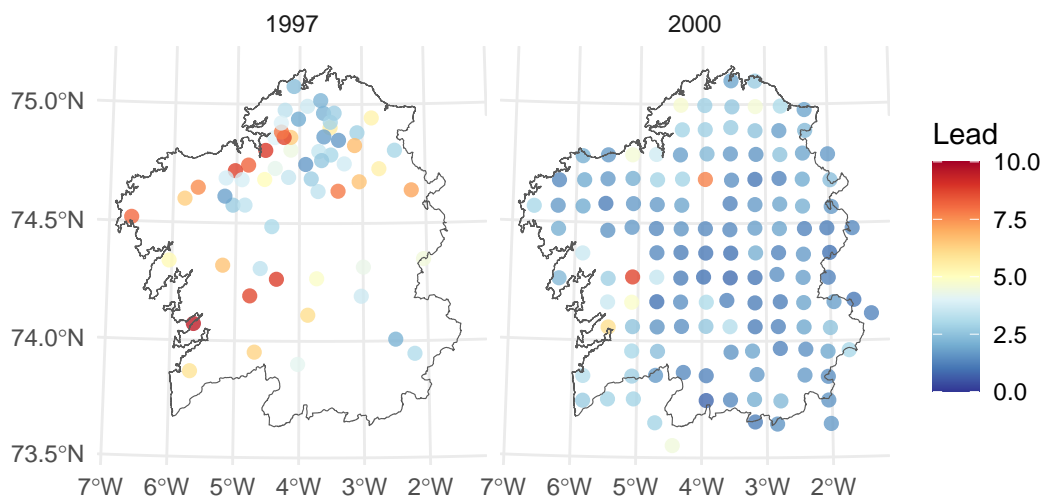


Figure 3: Observed lead concentrations at sampled locations in Galicia in 1997 and 2000.

5 Application to the Galicia moss data

The Galicia moss dataset has been a widely used example for illustrating the effects of preferential sampling on geostatistical inference and prediction (Diggle et al., 2010; Dinsdale and Salibián-Barrera, 2019). It contains lead concentrations in moss samples, measured in micrograms per gram of dry weight, collected from Galicia, northern Spain. Figure 3 shows the spatial distribution of 63 measurements taken in 1997 and 132 measurements taken in 2000. Sampling in 1997 was preferential, with a bias toward locations in the north with lower lead concentrations, whereas sampling in 2000 was more regular and non-preferential. Further details on the dataset can be found in Diggle et al. (2010).

We fit each of the MLE, INLA-SLP, ISIW-V, and ISIW-PM approaches using the 1997 and 2000 data separately and generated predictive surfaces over a 20×20 grid covering the Galicia area. Based on its good performance in the simulation analysis, we estimated the ISIW first stage intensities using `CvL.adaptive` bandwidth selection. We did encounter numerical difficulties when fitting the INLA-SPDE model to the 1997 data. While previous analyses of the Galicia dataset have used areal models, we elected to use the SPDE approach to be consistent with our simulation analysis. The model was particularly sensitive to the choice of prior for the range and initial value for the nugget. It would sometimes generate predictive surfaces with no variation, where the same value

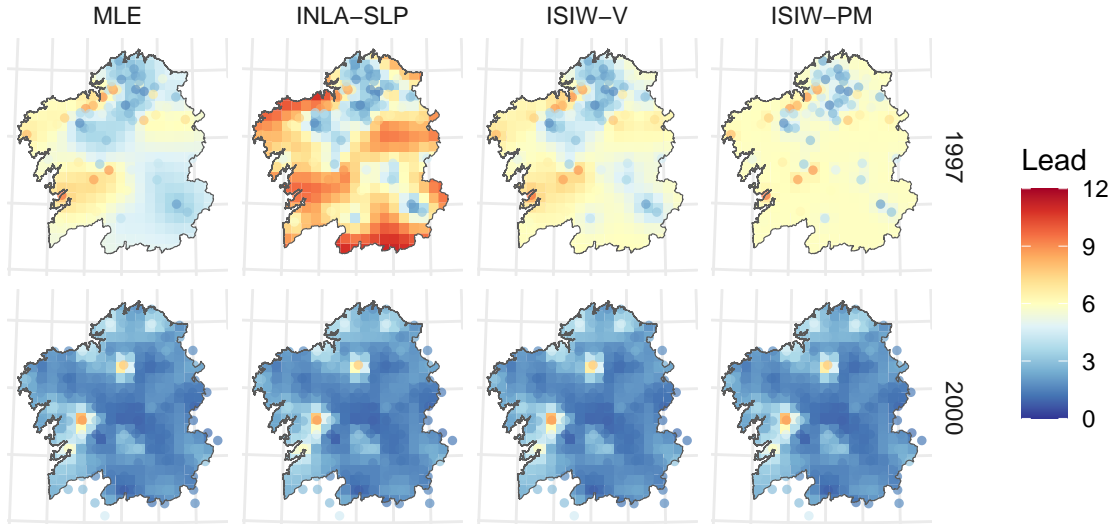


Figure 4: Spatial predictions of lead concentrations in Galicia in 1997 and 2000 using MLE, INLA-SLP, ISIW-V, and ISIW-PM. Points represent the observed data.

was predicted across the entire region including in locations with observations recording different values. Here we present the predictive surface that exhibited some variation and aligned with expectations from kriging, where predictions have similar values to the observations closeby.

Figure 4 displays the predictions for the lead concentration surface. There was little difference for the 2000 data, however, substantial differences emerged in the 1997 data. As expected, both the ISIW-V and INLA-SLP estimated higher values in data sparse areas to correct for the preferential sampling of low values. The INLA-SLP applied a more extreme correction than the ISIW-V, similar to the example in Figure 2. It unexpectedly predicted values exceeding 10.5 in the south, where the nearest observations fall below 5.00. It also estimated a very high μ of 10.79 (Table S5). This was unusual considering the maximum observation was 9.51 and the mean of all 63 observations in 1997 was 4.72. The MLE, ISIW-V, and ISIW-PM only estimated a μ of 5.15, 6.07, and 5.95, respectively. Besides being a result of INLA-SLP's PS adjustment, the discrepancy could also be attributed to numerical instability in INLA-SLP estimation, and other priors or initial values might produce different results.

Similar to our simulation results, the ISIW-PM estimated a lower range compared to other methods. This low range likely explains why its predictive surface exhibits little

spatial dependence with nearly uniform predictions across the region. ISIW-V appears to strike a balance between implementing a moderate adjustment for PS while preserving the spatial correlation evident in the dataset.

6 Discussion

In this work, we compared ISIW methods to the SLP and MLE for parameter estimation and prediction under preferential sampling. We implemented ISIW in a novel combination with the Vecchia approximation and found that, despite being less well-suited for geostatistical inference, ISIW with the Vecchia approximation nevertheless improves predictive accuracy over the MLE approach and remains competitive with the INLA-SLP approach using the true weights. We conducted a comprehensive simulation study that extended beyond previous analyses, evaluating the robustness of ISIW across various settings. Its benefits persisted across multiple observation point processes, different levels of spatial dependence in the underlying field, and alternative point process intensity estimators used in the first stage of ISIW. We also showed an application to the Galicia moss data where ISIW appears to give more reasonable predictions compared to the standard SLP approach.

Several factors make ISIW an attractive alternative to SLP for PS adjustment, namely its speed, simplicity, and strong predictive performance. Not only does it scale more efficiently with increasing n , but in terms of the practical implementation, we found that our version of ISIW-V ran faster than INLA-SLP for combined estimation and prediction, even though we did not implement an optimized version. ISIW is also simple to use and understand. INLA and TMB require specification of both the prior distributions for hyperparameters and mesh triangulation that can significantly alter results (Righetto et al., 2020). In contrast, ISIW is a straightforward inverse weighting method familiar to much of the research community that only requires an estimated vector of weights. Furthermore, since most effective Gaussian process approximation techniques are already based on the Vecchia approximation (Heaton et al., 2019), integrating ISIW into state-of-

the-art methods is significantly simpler and more straightforward compared to the SLP. These computational and conceptual advantages come without sacrificing predictive performance. In our simulation analysis, ISIW achieved improved predictive accuracy over the MLE with estimated weights and performed comparably to the gold standard SLP when the true weights were known. In scenarios where the SLP was misspecified, ISIW outperformed it, demonstrating greater robustness and fewer parametric assumptions.

Many improvements can still be made to ISIW. A significant gap remains between the predictive accuracy achieved by ISIW with estimated and true weights. The lack of accuracy and theoretical guarantees for the nonparametric intensity estimators used in this study may contribute to their inability to achieve similar performance. Moreover, Winsorization is necessary to prevent pathological numerical behavior but remains an undesirable ad hoc step. Intensity modelling incorporating the values of the observations rather than just their locations may also lead to improved weight estimation. Future work should explore more flexible and robust estimators for point process intensities beyond kernel density estimators and the INLA approach.

Additionally, ISIW does not yield reliable parameter estimates for the underlying geostatistical model. The weighted likelihood adjustment introduces substantial bias and error into parameter estimation, yet unexpectedly improves predictions through kriging. The apparent disconnect between parameter estimation and prediction warrants further investigation. It remains unclear why parameters obtained from the weighted likelihood adjustment consistently lead to better kriging predictions. While kriging is known to lose its predictive optimality under preferential sampling, the results of this study provide insight into conditions under which it can still serve as an effective function approximation tool under relaxed assumptions like PS.

Finally, we did not address uncertainty quantification for parameter estimates or predictions. While the kriging variance formula remains available and could be computed using the estimated parameters, its utility in the presence of preferential sampling is uncertain. In addition, geostatistical inference is already challenging and preferential sampling adjustment appears to exacerbate the difficulty. As a result, any standard

errors for parameter estimates obtained under ISIW are unlikely to have valid coverage properties. Future work will focus on developing principled approaches to quantifying uncertainty in both inference and prediction under ISIW.

7 Supplementary Material

Table S1: Average RMSPE (standard deviation) for methods under the LGCP simulation. Bolded values indicate the method with the lowest average RMSPE across all simulations for that setting.

Method	Weights	N = 100		N = 800	
		$\phi = 0.02$	$\phi = 0.15$	$\phi = 0.02$	$\phi = 0.15$
MLE		1.726 (0.11)	0.785 (0.17)	1.306 (0.06)	0.361 (0.07)
INLA-SLP		1.195 (0.08)	0.553 (0.09)	0.995 (0.04)	0.305 (0.04)
ISIW-V	Known	1.193 (0.11)	0.656 (0.13)	0.908 (0.04)	0.346 (0.06)
	CvL	1.660 (0.12)	0.728 (0.16)	1.238 (0.06)	0.353 (0.06)
	CvL.adaptive	1.639 (0.18)	0.714 (0.20)	1.098 (0.07)	0.362 (0.07)
	INLA	1.686 (0.11)	0.783 (0.17)	1.204 (0.05)	0.355 (0.06)
	diggle	1.616 (0.18)	0.712 (0.19)	1.112 (0.14)	0.355 (0.07)
	ppl	1.664 (0.13)	0.730 (0.23)	1.168 (0.16)	0.361 (0.13)
	scott	1.689 (0.11)	0.737 (0.20)	1.279 (0.06)	0.353 (0.06)
ISIW-PM	Known	1.210 (0.10)	0.773 (0.18)	1.066 (0.06)	0.384 (0.08)
	CvL	1.736 (0.12)	0.846 (0.21)	1.390 (0.07)	0.390 (0.09)
	CvL.adaptive	1.614 (0.16)	0.766 (0.18)	1.175 (0.06)	0.395 (0.09)
	INLA	1.764 (0.12)	1.006 (0.26)	1.331 (0.06)	0.392 (0.09)
	diggle	1.593 (0.16)	0.774 (0.19)	1.136 (0.06)	0.382 (0.08)
	ppl	1.723 (0.13)	0.804 (0.18)	1.238 (0.06)	0.380 (0.08)
	scott	1.788 (0.12)	0.845 (0.19)	1.448 (0.07)	0.393 (0.09)

Table S2: Average RMSPE (standard deviation) for methods under the SCP simulation. Bolded values indicate the method with the lowest average RMSPE across all simulations for that setting.

Method	Weights	N = 100		N = 800	
		$\phi = 0.02$	$\phi = 0.15$	$\phi = 0.02$	$\phi = 0.15$
MLE		1.289 (0.06)	0.579 (0.10)	0.999 (0.04)	0.271 (0.03)
INLA-SLP		1.374 (0.31)	0.521 (0.08)	0.935 (0.03)	0.258 (0.02)
ISIW-V	Known	1.228 (0.08)	0.551 (0.08)	0.889 (0.03)	0.270 (0.03)
	CvL	1.280 (0.07)	0.566 (0.09)	0.975 (0.04)	0.268 (0.03)
	CvL.adaptive	1.292 (0.09)	0.574 (0.09)	0.941 (0.05)	0.272 (0.03)
	INLA	1.289 (0.07)	0.581 (0.10)	0.984 (0.04)	0.270 (0.03)
	diggle	1.286 (0.08)	0.570 (0.10)	0.976 (0.04)	0.268 (0.03)
	ppl	1.288 (0.06)	0.569 (0.09)	0.987 (0.04)	0.269 (0.03)
	scott	1.285 (0.06)	0.568 (0.09)	0.995 (0.04)	0.269 (0.03)
ISIW-PM	Known	1.232 (0.09)	0.596 (0.11)	0.900 (0.03)	0.281 (0.03)
	CvL	1.287 (0.07)	0.612 (0.12)	1.017 (0.04)	0.281 (0.04)
	CvL.adaptive	1.287 (0.10)	0.609 (0.12)	0.964 (0.04)	0.278 (0.03)
	INLA	1.298 (0.07)	0.660 (0.14)	1.020 (0.04)	0.287 (0.04)
	diggle	1.282 (0.08)	0.601 (0.11)	1.017 (0.04)	0.281 (0.04)
	ppl	1.303 (0.06)	0.630 (0.12)	1.033 (0.04)	0.283 (0.04)
	scott	1.296 (0.06)	0.628 (0.12)	1.043 (0.04)	0.285 (0.04)

Table S3: Average RMSPE (standard deviation) for methods under the Thomas process simulation. Bolded values indicate the method with the lowest average RMSPE across all simulations for that setting.

Method	Weights	N = 100		N = 800	
		$\phi = 0.02$	$\phi = 0.15$	$\phi = 0.02$	$\phi = 0.15$
MLE		1.684 (0.11)	0.822 (0.20)	1.324 (0.06)	0.376 (0.07)
INLA-SLP		1.214 (0.11)	0.749 (0.27)	0.983 (0.04)	0.324 (0.07)
ISIW-V	Known	1.207 (0.11)	0.694 (0.15)	0.918 (0.06)	0.359 (0.06)
	CvL	1.641 (0.14)	0.765 (0.18)	1.265 (0.06)	0.367 (0.07)
	CvL.adaptive	1.627 (0.20)	0.752 (0.18)	1.121 (0.09)	0.375 (0.07)
	INLA	1.629 (0.12)	0.812 (0.20)	1.216 (0.06)	0.369 (0.07)
	diggle	1.580 (0.18)	0.766 (0.20)	1.137 (0.14)	0.367 (0.07)
	ppl	1.682 (0.26)	0.909 (0.41)	1.278 (0.28)	0.412 (0.25)
	scott	1.644 (0.13)	0.772 (0.24)	1.294 (0.06)	0.367 (0.07)
ISIW-PM	Known	1.217 (0.08)	0.816 (0.21)	1.067 (0.06)	0.403 (0.09)
	CvL	1.744 (0.15)	0.918 (0.28)	1.435 (0.08)	0.414 (0.11)
	CvL.adaptive	1.603 (0.17)	0.816 (0.21)	1.182 (0.07)	0.409 (0.10)
	INLA	1.720 (0.12)	1.040 (0.28)	1.337 (0.06)	0.411 (0.10)
	diggle	1.558 (0.16)	0.830 (0.22)	1.168 (0.07)	0.397 (0.09)
	ppl	1.617 (0.18)	0.816 (0.21)	1.239 (0.07)	0.397 (0.09)
	scott	1.762 (0.13)	0.886 (0.22)	1.482 (0.08)	0.413 (0.10)

Table S4: Mean (SD) and Median (IQR) runtime in seconds over all simulations for methods under different sample sizes.

Method	Variant	N = 100		N = 800	
		Mean (SD)	Median (IQR)	Mean (SD)	Median (IQR)
MLE		0.80 (0.26)	0.76 (0.34)	43.8 (13.8)	41.3 (17.2)
INLA-SLP		124.0 (71.8)	100.0 (87.3)	99.8 (39.3)	95.2 (37.3)
ILIW	Known	4.80 (1.81)	4.47 (2.20)	45.8 (16.5)	43.3 (20.9)
	CvL	4.14 (1.48)	3.85 (1.89)	34.4 (10.7)	32.7 (13.6)
	CvL.adaptive	4.97 (1.75)	4.63 (2.11)	41.6 (13.7)	39.4 (17.5)
	INLA	15.9 (4.51)	15.0 (5.39)	118.0 (41.4)	107.0 (51.0)
	diggle	4.83 (1.93)	4.44 (2.24)	42.5 (17.3)	39.1 (22.1)
	ppl	4.88 (1.89)	4.49 (2.16)	39.3 (16.2)	36.0 (16.8)
	scott	4.08 (1.44)	3.79 (1.83)	34.3 (11.0)	32.6 (13.8)
PMLE	Known	0.26 (0.06)	0.25 (0.06)	16.5 (2.4)	16.2 (3.3)
	CvL	0.25 (0.05)	0.24 (0.05)	14.9 (2.1)	14.8 (2.8)
	CvL.adaptive	0.59 (0.14)	0.55 (0.15)	16.6 (2.1)	16.4 (2.9)
	INLA	9.61 (3.90)	8.40 (3.41)	97.4 (36.4)	86.3 (41.8)
	diggle	0.28 (0.06)	0.27 (0.06)	16.4 (2.3)	16.2 (3.2)
	ppl	0.65 (0.13)	0.64 (0.18)	15.7 (2.1)	15.6 (2.8)
	scott	0.25 (0.05)	0.25 (0.05)	15.0 (2.3)	14.8 (3.3)

Table S5: Parameter estimates for the Galicia data.

Year	Method	μ	σ^2	ϕ (km)	τ^2
1997	MLE	5.15	2.85	15.35	2.24
	INLA-SLP	10.79	18.19	17.54	0.00007
	ISIW-V	6.07	2.18	8.45	1.04
	ISIW-PM	5.95	1.24	3.99	2.08
2000	MLE	2.24	1.40	8.90	0.000
	INLA-SLP	2.27	1.36	10.2	0.00013
	ISIW-V	2.24	1.40	8.91	0.000
	ISIW-PM	2.15	1.37	9.47	0.016

References

- Amaral, A. V. R., Krainski, E. T., Zhong, R., and Moraga, P. (2023). Model-Based Geostatistics Under Spatially Varying Preferential Sampling. *Journal of Agricultural, Biological and Environmental Statistics*.
- Bachoc, F. (2014). Asymptotic analysis of the role of spatial sampling for covariance parameter estimation of Gaussian processes. *Journal of Multivariate Analysis*, 125:1–35.
- Bachoc, F. (2020). Asymptotic analysis of maximum likelihood estimation of covariance parameters for Gaussian processes: an introduction with proofs. arXiv:2009.07002 [math].
- Bachoc, F., Bevilacqua, M., and Velandia, D. (2019). Composite likelihood estimation for a Gaussian process under fixed domain asymptotics. *Journal of Multivariate Analysis*, 174:104534.
- Berman, M. and Diggle, P. (1989). Estimating Weighted Integrals of the Second-Order Intensity of a Spatial Point Process. *Journal of the Royal Statistical Society. Series B (Methodological)*, 51(1):81–92. Publisher: [Royal Statistical Society, Wiley].
- Bevilacqua, M. and Gaetan, C. (2015). Comparing composite likelihood methods based on pairs for spatial Gaussian random fields. *Statistics and Computing*, 25(5):877–892.
- Bolin, D. and Wallin, J. (2024). Spatial confounding under infill asymptotics. arXiv:2403.18961 [math].
- Cecconi, L., Biggeri, A., Grisotto, L., Berrocal, V., Rinaldi, L., Musella, V., Cringoli, G., and Catelan, D. (2016). Preferential sampling in veterinary parasitological surveillance. *Geospatial Health*, 11(1). Number: 1.
- Conn, P. B., Thorson, J. T., and Johnson, D. S. (2017). Confronting preferential sampling when analysing population distributions: diagnosis and model-

- based triage. *Methods in Ecology and Evolution*, 8(11):1535–1546. _eprint: <https://besjournals.onlinelibrary.wiley.com/doi/pdf/10.1111/2041-210X.12803>.
- Conroy, B., Waller, L. A., Buller, I. D., Hacker, G. M., Tucker, J. R., and Novak, M. G. (2023). A Shared Latent Process Model to Correct for Preferential Sampling in Disease Surveillance Systems. *Journal of Agricultural, Biological and Environmental Statistics*, 28(3):483–501.
- Cressie, N. and Wikle, C. K. (2015). *Statistics for Spatio-Temporal Data*. John Wiley & Sons. Google-Books-ID: 4L_dCgAAQBAJ.
- Cronie, O. and Van Lieshout, M. N. M. (2018). A non-model-based approach to bandwidth selection for kernel estimators of spatial intensity functions. *Biometrika*, 105(2):455–462.
- Datta, A., Banerjee, S., Finley, A. O., and Gelfand, A. E. (2016). Hierarchical Nearest-Neighbor Gaussian Process Models for Large Geostatistical Datasets. *Journal of the American Statistical Association*, 111(514):800–812. Publisher: Taylor & Francis _eprint: <https://doi.org/10.1080/01621459.2015.1044091>.
- Diggle, P. (1985). A Kernel Method for Smoothing Point Process Data. *Journal of the Royal Statistical Society: Series C (Applied Statistics)*, 34(2):138–147. _eprint: <https://onlinelibrary.wiley.com/doi/pdf/10.2307/2347366>.
- Diggle, P. J., Menezes, R., and Su, T.-l. (2010). Geostatistical inference under preferential sampling. *Journal of the Royal Statistical Society: Series C (Applied Statistics)*, 59(2):191–232. _eprint: <https://rss.onlinelibrary.wiley.com/doi/pdf/10.1111/j.1467-9876.2009.00701.x>.
- Diggle, P. J., Tawn, J. A., and Moyeed, R. A. (1998). Model-based geostatistics. *Journal of the Royal Statistical Society: Series C (Applied Statistics)*, 47(3):299–350. _eprint: <https://rss.onlinelibrary.wiley.com/doi/pdf/10.1111/1467-9876.00113>.

- Dinsdale, D. and Salibian-Barrera, M. (2019). Methods for preferential sampling in geostatistics. *Journal of the Royal Statistical Society: Series C (Applied Statistics)*, 68(1):181–198. _eprint: <https://onlinelibrary.wiley.com/doi/pdf/10.1111/rssc.12286>.
- Fandos, G., Kéry, M., Cano-Alonso, L. S., Carbonell, I., and Luis Tellería, J. (2021). Dynamic multistate occupancy modeling to evaluate population dynamics under a scenario of preferential sampling. *Ecosphere*, 12(4):e03469. _eprint: <https://onlinelibrary.wiley.com/doi/pdf/10.1002/ecs2.3469>.
- Ferreira, G. d. S. (2020). Geostatistics under preferential sampling in the presence of local repulsion effects. *Environmental and Ecological Statistics*, 27(3):549–570.
- Ferreira, G. d. S. and Gamerman, D. (2015). Optimal Design in Geostatistics under Preferential Sampling. *Bayesian Analysis*, 10(3):711–735. Publisher: International Society for Bayesian Analysis.
- Fithian, W., Elith, J., Hastie, T., and Keith, D. A. (2015). Bias correction in species distribution models: pooling survey and collection data for multiple species. *Methods in Ecology and Evolution*, 6(4):424–438. _eprint: <https://onlinelibrary.wiley.com/doi/pdf/10.1111/2041-210X.12242>.
- Fuglstad, G.-A., Simpson, D., Lindgren, F., and Rue, H. (2019). Constructing Priors that Penalize the Complexity of Gaussian Random Fields. *Journal of the American Statistical Association*, 114(525):445–452.
- Gelfand, A. E., Diggle, P., Guttorp, P., and Fuentes, M. (2010). *Handbook of Spatial Statistics*. Taylor & Francis Group, Milton, UNITED KINGDOM.
- Gelfand, A. E., Sahu, S. K., and Holland, D. M. (2012). On the effect of preferential sampling in spatial prediction. *Environmetrics*, 23(7):565–578. _eprint: <https://onlinelibrary.wiley.com/doi/pdf/10.1002/env.2169>.
- Gelfand, A. E. and Shirota, S. (2019). Preferential sampling for presence/absence data and for fusion of presence/absence data with

- presence-only data. *Ecological Monographs*, 89(3):e01372. [_eprint: https://onlinelibrary.wiley.com/doi/pdf/10.1002/ecm.1372.](https://onlinelibrary.wiley.com/doi/pdf/10.1002/ecm.1372)
- Gilbert, B., Ogburn, E. L., and Datta, A. (2024). Consistency of common spatial estimators under spatial confounding. *Biometrika*, page asae070.
- Gray, E. J. and Evangelou, E. (2023). A design utility approach for preferentially sampled spatial data. *Journal of the Royal Statistical Society Series C: Applied Statistics*, 72(4):1041–1063.
- Guan, Y. (2008). On Consistent Nonparametric Intensity Estimation for Inhomogeneous Spatial Point Processes. *Journal of the American Statistical Association*, 103(483):1238–1247.
- Guinness, J. (2018). Permutation and Grouping Methods for Sharpening Gaussian Process Approximations. *Technometrics*, 60(4):415–429. Publisher: Taylor & Francis [_eprint: https://doi.org/10.1080/00401706.2018.1437476.](https://doi.org/10.1080/00401706.2018.1437476)
- Guinness, J. (2021). Gaussian process learning via Fisher scoring of Vecchia’s approximation. *Statistics and Computing*, 31(3):25.
- Heaton, M. J., Datta, A., Finley, A. O., Furrer, R., Guinness, J., Guhaniyogi, R., Gerber, F., Gramacy, R. B., Hammerling, D., Katzfuss, M., Lindgren, F., Nychka, D. W., Sun, F., and Zammit-Mangion, A. (2019). A Case Study Competition Among Methods for Analyzing Large Spatial Data. *Journal of Agricultural, Biological and Environmental Statistics*, 24(3):398–425.
- Ho, L. P. and Stoyan, D. (2008). Modelling marked point patterns by intensity-marked Cox processes. *Statistics & Probability Letters*, 78(10):1194–1199.
- Huser, R., Stein, M. L., and Zhong, P. (2023). Vecchia Likelihood Approximation for Accurate and Fast Inference with Intractable Spatial Max-Stable Models. *Journal of Computational and Graphical Statistics*, 0(0):1–22. Publisher: Taylor & Francis [_eprint: https://doi.org/10.1080/10618600.2023.2285332.](https://doi.org/10.1080/10618600.2023.2285332)

- Karcher, M. D., Palacios, J. A., Bedford, T., Suchard, M. A., and Minin, V. N. (2016). Quantifying and Mitigating the Effect of Preferential Sampling on Phylodynamic Inference. *PLoS Computational Biology*, 12(3):e1004789. Publisher: Public Library of Science.
- Katzfuss, M. and Guinness, J. (2021). A General Framework for Vecchia Approximations of Gaussian Processes. *Statistical Science*, 36(1):124–141. Publisher: Institute of Mathematical Statistics.
- Katzfuss, M., Guinness, J., Gong, W., and Zilber, D. (2020). Vecchia Approximations of Gaussian-Process Predictions. *Journal of Agricultural, Biological and Environmental Statistics*, 25(3):383–414.
- Kaufman, C. G. and Shaby, B. A. (2013). The role of the range parameter for estimation and prediction in geostatistics. *Biometrika*, 100(2):473–484.
- Kristensen, K., Nielsen, A., Berg, C. W., Skaug, H., and Bell, B. M. (2016). TMB: Automatic Differentiation and Laplace Approximation. *Journal of Statistical Software*, 70:1–21.
- Lee, A., Szpiro, A., Kim, S. Y., and Sheppard, L. (2015). Impact of preferential sampling on exposure prediction and health effect inference in the context of air pollution epidemiology. *Environmetrics*, 26(4):255–267. _eprint: <https://onlinelibrary.wiley.com/doi/pdf/10.1002/env.2334>.
- Lee, D., Ferguson, C., and Scott, E. M. (2011). Constructing representative air quality indicators with measures of uncertainty. *Journal of the Royal Statistical Society: Series A (Statistics in Society)*, 174(1):109–126. _eprint: <https://rss.onlinelibrary.wiley.com/doi/pdf/10.1111/j.1467-985X.2010.00658.x>.
- Lindgren, F., Rue, H., and Lindström, J. (2011). An explicit link between Gaussian fields and Gaussian Markov random fields: the stochastic partial differential equation approach. *Journal of the Royal Statistical Society: Series B (Statistical Methodol-*

- ogy*), 73(4):423–498. [_eprint: https://onlinelibrary.wiley.com/doi/pdf/10.1111/j.1467-9868.2011.00777.x](https://onlinelibrary.wiley.com/doi/pdf/10.1111/j.1467-9868.2011.00777.x).
- Loader, C. (1999). Density Estimation. In Loader, C., editor, *Local Regression and Likelihood*, Statistics and Computing, pages 79–100. Springer, New York, NY.
- Loh, W.-L., Sun, S., and Wen, J. (2021). On fixed-domain asymptotics, parameter estimation and isotropic Gaussian random fields with Matérn covariance functions. *The Annals of Statistics*, 49(6).
- Manceur, A. M. and Kühn, I. (2014). Inferring model-based probability of occurrence from preferentially sampled data with uncertain absences using expert knowledge. *Methods in Ecology and Evolution*, 5(8):739–750. [_eprint: https://onlinelibrary.wiley.com/doi/pdf/10.1111/2041-210X.12224](https://onlinelibrary.wiley.com/doi/pdf/10.1111/2041-210X.12224).
- Mardia, K. V. and Marshall, R. J. (1984). Maximum Likelihood Estimation of Models for Residual Covariance in Spatial Regression. *Biometrika*, 71(1):135–146. Publisher: [Oxford University Press, Biometrika Trust].
- Moreira, G. A. and Gamerman, D. (2022). Analysis of presence-only data via exact Bayes, with model and effects identification. *The Annals of Applied Statistics*, 16(3):1848–1867. Publisher: Institute of Mathematical Statistics.
- Moreira, G. A., Menezes, R., and Wise, L. (2023). Presence-Only for Marked Point Process Under Preferential Sampling. *Journal of Agricultural, Biological and Environmental Statistics*.
- Paci, L., Gelfand, A. E., Beamonte, a. M. A., Gargallo, P., and Salvador, M. (2020). Spatial hedonic modelling adjusted for preferential sampling. *Journal of the Royal Statistical Society: Series A (Statistics in Society)*, 183(1):169–192. [_eprint: https://rss.onlinelibrary.wiley.com/doi/pdf/10.1111/rssa.12489](https://rss.onlinelibrary.wiley.com/doi/pdf/10.1111/rssa.12489).
- Pati, D., Reich, B. J., and Dunson, D. B. (2011). Bayesian geostatistical modelling with informative sampling locations. *Biometrika*, 98(1):35–48.

- Pennino, M. G., Paradinas, I., Illian, J. B., Muñoz, F., Bellido, J. M., López-Quílez, A., and Conesa, D. (2019). Accounting for preferential sampling in species distribution models. *Ecology and Evolution*, 9(1):653–663. _eprint: <https://onlinelibrary.wiley.com/doi/pdf/10.1002/ece3.4789>.
- Putter, H. and Young, G. A. (2001). On the Effect of Covariance Function Estimation on the Accuracy of Kriging Predictors. *Bernoulli*, 7(3):421–438. Publisher: International Statistical Institute (ISI) and Bernoulli Society for Mathematical Statistics and Probability.
- Reich, B. J. and Fuentes, M. (2012). Accounting for Design in the Analysis of Spatial Data. In Mateu, J. and Müller, W. G., editors, *Spatio-Temporal Design*, pages 131–141. John Wiley & Sons, Ltd, Chichester, UK.
- Righetto, A. J., Faes, C., Vandendijck, Y., and Ribeiro, P. J. (2020). On the choice of the mesh for the analysis of geostatistical data using R-INLA. *Communications in Statistics - Theory and Methods*, 49(1):203–220. Publisher: Taylor & Francis _eprint: <https://doi.org/10.1080/03610926.2018.1536209>.
- Rinaldi, L., Biggeri, A., Musella, V., Waal, T. d., Hertzberg, H., Mavrot, F., Torgerson, P. R., Selemetas, N., Coll, T., Bosco, A., Grisotto, L., Cringoli, G., and Catelan, D. (2015). Sheep and Fasciola hepatica in Europe: the GLOWORM experience. *Geospatial Health*, 9(2):309–317. Number: 2.
- Rue, H., Martino, S., and Chopin, N. (2009). Approximate Bayesian inference for latent Gaussian models by using integrated nested Laplace approximations. *Journal of the Royal Statistical Society: Series B (Statistical Methodology)*, 71(2):319–392. _eprint: <https://rss.onlinelibrary.wiley.com/doi/pdf/10.1111/j.1467-9868.2008.00700.x>.
- Schlather, M., Ribeiro Jr, P. J., and Diggle, P. J. (2004). Detecting dependence between marks and locations of marked point processes. *Journal of the Royal Statistical Society: Series B (Statistical Methodology)*, 66(1):79–93. _eprint: <https://onlinelibrary.wiley.com/doi/pdf/10.1046/j.1369-7412.2003.05343.x>.

- Schliep, E. M., Wikle, C. K., and Daw, R. (2023). Correcting for informative sampling in spatial covariance estimation and kriging predictions. *Journal of Geographical Systems*.
- Scott, D. (1992). Kernel Density Estimators. In *Multivariate Density Estimation*, pages 125–193. John Wiley & Sons, Ltd. Section: 6. eprint: <https://onlinelibrary.wiley.com/doi/pdf/10.1002/9780470316849.ch6>.
- Shirota, S. and Gelfand, A. E. (2022). Preferential sampling for bivariate spatial data. *Spatial Statistics*, 51:100674.
- Simpson, D., Illian, J. B., Lindgren, F., Sørbye, S. H., and Rue, H. (2016). Going off grid: computationally efficient inference for log-Gaussian Cox processes. *Biometrika*, 103(1):49–70.
- Simpson, D., Rue, H., Riebler, A., Martins, T. G., and Sørbye, S. H. (2017). Penalising Model Component Complexity: A Principled, Practical Approach to Constructing Priors. *Statistical Science*, 32(1):1–28. Publisher: Institute of Mathematical Statistics.
- Stein, M. (1990a). Uniform Asymptotic Optimality of Linear Predictions of a Random Field Using an Incorrect Second-Order Structure. *The Annals of Statistics*, 18(2):850–872. Publisher: Institute of Mathematical Statistics.
- Stein, M. L. (1988). Asymptotically Efficient Prediction of a Random Field with a Misspecified Covariance Function. *The Annals of Statistics*, 16(1):55–63. Publisher: Institute of Mathematical Statistics.
- Stein, M. L. (1990b). Bounds on the Efficiency of Linear Predictions Using an Incorrect Covariance Function. *The Annals of Statistics*, 18(3):1116–1138. Publisher: Institute of Mathematical Statistics.
- Stein, M. L. (1993). A simple condition for asymptotic optimality of linear predictions of random fields. *Statistics & Probability Letters*, 17(5):399–404.
- Tang, W., Zhang, L., and Banerjee, S. (2021). On Identifiability and Consistency of The

- Nugget in Gaussian Spatial Process Models. *Journal of the Royal Statistical Society Series B: Statistical Methodology*, 83(5):1044–1070.
- van Lieshout, M. (2021). Infill asymptotics for adaptive kernel estimators of spatial intensity. *Australian & New Zealand Journal of Statistics*, 63(1):159–181. [_eprint: https://onlinelibrary.wiley.com/doi/pdf/10.1111/anzs.12319](https://onlinelibrary.wiley.com/doi/pdf/10.1111/anzs.12319).
- Varin, C., Reid, N., and Firth, D. (2011). An Overview of Composite Likelihood Methods. *Statistica Sinica*, 21(1):5–42. Publisher: Institute of Statistical Science, Academia Sinica.
- Vecchia, A. V. (1988). Estimation and Model Identification for Continuous Spatial Processes. *Journal of the Royal Statistical Society. Series B (Methodological)*, 50(2):297–312. Publisher: [Royal Statistical Society, Wiley].
- Vedensky, D., Parker, P. A., and Holan, S. H. (2023). A Look into the Problem of Preferential Sampling through the Lens of Survey Statistics. *The American Statistician*, 77(3):313–322. Publisher: Taylor & Francis [_eprint: https://doi.org/10.1080/00031305.2022.2143898](https://doi.org/10.1080/00031305.2022.2143898).
- Wang, W., Tuo, R., and Jeff Wu, C. F. (2020). On Prediction Properties of Kriging: Uniform Error Bounds and Robustness. *Journal of the American Statistical Association*, 115(530):920–930. Publisher: Taylor & Francis [_eprint: https://doi.org/10.1080/01621459.2019.1598868](https://doi.org/10.1080/01621459.2019.1598868).
- Watson, J. (2021). A perceptron for detecting the preferential sampling of locations and times chosen to monitor a spatio-temporal process. *Spatial Statistics*, 43:100500.
- Watson, J., Zidek, J. V., and Shaddick, G. (2019). A general theory for preferential sampling in environmental networks. *The Annals of Applied Statistics*, 13(4):2662–2700. Publisher: Institute of Mathematical Statistics.
- Yu, N. (2022). *Parametric Estimation in Spatial Regression Models*. PhD thesis, University of Maryland, College Park.

- Zhang, H. (2004). Inconsistent Estimation and Asymptotically Equal Interpolations in Model-Based Geostatistics. *Journal of the American Statistical Association*, 99(465):250–261.
- Zhang, L., Tang, W., and Banerjee, S. (2024). Fixed-Domain Asymptotics Under Vecchia’s Approximation of Spatial Process Likelihoods. *Statistica Sinica*, 34(4):1863–1881.
- Zidek, J. V., Shaddick, G., and Taylor, C. G. (2014). Reducing estimation bias in adaptively changing monitoring networks with preferential site selection. *The Annals of Applied Statistics*, 8(3):1640–1670. Publisher: Institute of Mathematical Statistics.